

1 Modelled glacier equilibrium line altitudes during the mid- 2 Holocene in the southern mid-latitudes

3
4 **C. Bravo**^{1,2,3,*}, **M. Rojas**^{1,2,3}, **B. M. Anderson**⁴, **A. N. Mackintosh**⁴, **E. Sagredo**^{3,5}
5 **and P.I. Moreno**^{2,3,6}

6 [1]{Department of Geophysics, Universidad de Chile, Santiago, Chile}

7 [2]{Center for Climate and Resilience Research (CR2), Universidad de Chile, Santiago
8 Chile}

9 [3]{Millennium Nucleus Paleoclimate of the Southern Hemisphere, Santiago, Chile}

10 [4]{Antarctic Research Centre, Victoria University of Wellington, Wellington, New
11 Zealand}

12 [5] {Institute of Geography, Pontificia Universidad Católica de Chile, Santiago, Chile}

13 [6]{Department of Ecological Sciences and Institute of Ecology and Biodiversity,
14 Universidad de Chile, Santiago, Chile}

15 [*]{Now at Glaciology Laboratory, Centro de Estudios Científicos, Valdivia, Chile}

16 Correspondence to: Claudio Bravo (claudio@dgf.uchile.cl)

17 18 **Abstract**

19 Glacier behaviour during the Mid-Holocene (MH, 6000 year B.P.) in the Southern
20 Hemisphere provides observational data to constrain our understanding of the origin and
21 propagation of paleoclimate signals. In this study we examine the climatic forcing of
22 glacier response in the MH by evaluating modelled glacier equilibrium line altitudes
23 (ELAs) and climatic conditions during the MH compared with pre-industrial time (PI, year
24 1750). We focus on the middle latitudes of the Southern Hemisphere, specifically Patagonia
25 and the South Island of New Zealand. Climate conditions for the MH were obtained from
26 PMIP2 models simulations, which in turn were used to force a simple glacier mass balance
27 model to simulate changes in ELA. In Patagonia, the models simulate colder conditions
28 during the MH in the austral summer (-0.2°C), autumn (-0.5°C) and winter (-0.4), and

1 warmer temperatures (0.2°C) during spring. In the Southern Alps the models show colder
2 MH condition in autumn (-0.7°C) and winter (-0.4°C) warmer conditions in spring (0.3°C)
3 and no significant change in summer temperature.

4 Precipitation does not show significant changes, but exhibits a seasonal shift with less
5 precipitation from April to September and more precipitation from October to April during
6 the MH in both regions. The mass balance model simulates a climatic ELA that is 15 - 33
7 m lower during the MH compared with PI conditions. We suggest that the main causes of
8 this difference are driven mainly by colder temperatures associated to the MH simulation.
9 Differences in temperature have a dual effect on glacier mass balance: (i) less energy is
10 available for ablation during summer and early autumn and (ii) lower temperatures cause
11 more precipitation to fall as snow rather than rain in late autumn and winter, resulting in
12 more accumulation and higher surface albedo. For these reasons, we postulate that the
13 modelled ELA changes, although small, may help to explain larger glacier extents observed
14 by 6000 yr B.P. in South America and New Zealand.

15

16 **1 Introduction**

17 Deciphering the climate signals and glacial history of the mid-latitudes of the Southern
18 Hemisphere (Fig. 1) during the Holocene is key to unravelling the mechanism of climate
19 change that occurred during this period. During the last ~11500 years, a series of intervals
20 of rapid climate changes occurred worldwide (Mayewski et al., 2004). Reduction in
21 temperature and/or increases in precipitation during these periods have been recorded as
22 multiple glacial advances in different areas of the planet. Solomina et al. (2015) recently
23 provided a global review of Holocene glacier activity. Periods of renewed glacial activity,
24 known as Neoglaciations (Porter and Denton, 1967), were initially identified in the
25 Northern Hemisphere. However, during the last decades, numerous studies have shown
26 evidence of glacial advances, as well as climate variability during this period in the
27 Southern Hemisphere (approximately between 35° to 55° S). Most of these studies have
28 focused on Patagonia (e.g. Clapperton and Sugden, 1988; Porter, 2000; Rodbell et al.,
29 2009; Strelin et al., 2014) and in the Southern Alps in New Zealand (e.g. Gellatly et al.,
30 1988; Porter, 2000; Schaefer et al., 2009, Putnam et al. 2012, Kaplan et al. 2013).

1 In Patagonia (Fig. 1), a number of different Neoglacial chronologies have been produced
2 (e.g. Mercer, 1982; Aniya, 1995; Clapperton and Sugden, 1988; Aniya, 2013). However,
3 significant differences between these chronologies have not been fully resolved.

4 In Southern Island of New Zealand (Fig. 1), on the other hand, notable periods of glacier
5 still stand or re-advance occurred during the early to mid-Holocene, as well as during the
6 last millennium (Schaefer et al. 2009, Putnam et al 2012). It appears that these centennial-
7 scale glacial events have been superimposed on a long-term trend of decreasing ice extent
8 that persisted for the entire Holocene (Schaefer et al. 2009, Putnam et al. 2012, Kaplan et
9 al. 2013).

10 In this context, it is clear that several aspects of the Neoglacial chronology of the southern
11 mid-latitudes (35°-55°S) are still inadequately understood, and more detailed chronologies
12 are needed. Particularly relevant for this study is the lack of agreement regarding the timing
13 of the Neoglaciations in the southern mid-latitudes (Porter, 2000).

14 Understanding the climate and glacial history of the southern mid-latitudes is a prerequisite
15 for testing hypotheses regarding the origin and propagation of palaeoclimate signals, the
16 coupling of the ocean–atmosphere in the extra-tropics, and the interaction of low- and high-
17 latitude climate controls on hemispheric and global climate (Fletcher and Moreno, 2012,
18 Moreno et al., 2010, Rojas et al. 2009, Putnam et al. 2012). The mid-Holocene represents a
19 key moment in our late climate history. This period, within the current interglacial cycle
20 had important differences in orbital parameters with respect to the present conditions and
21 was devoid of influences from late-glacial climate change (Braconnot et al., 2007).
22 Although recent work has demonstrated that orbital forcing may not have played a critical
23 role in glacier behavior during cold phases of the last glacial cycle (Doughty et al., 2015),
24 the climatic boundary conditions at that time were very different than during the Holocene.
25 Considering the uncertainty in the timing of the beginning of the Neoglaciation, but that
26 geologic evidence suggest that glaciers were larger than present between 8000-6000 yr B.P.
27 in both regions (Kaplan et al., 2013, Schaefer et al., 2009, Putnam et al., 2012, Douglass et
28 al., 2005, Harrison et al., 2012), the aim of this work is to undertake a first-order modelling
29 study to assess if the climatic conditions during the mid-Holocene would permit the
30 existence of more extensive glaciers than during the Pre-Industrial (PI) period. The PI

1 periods was chosen as the reference period instead of 20th Century climate because of
2 availability of modeling output to drive the mass balance model.

3 At the mid-Holocene (MH hereafter), orbital differences resulted negative insolation
4 anomalies from November through March and positive anomalies from June to October in
5 southern mid-latitudes (Rojas and Moreno, 2011). We expect that these orbital/insolation
6 differences had a major impact on the glacial extent and especially in the equilibrium line
7 altitudes (ELA) of glaciers. The equilibrium line altitude is a climatic sensitive parameter
8 marking the location on a glacier where accumulation of snow is exactly balanced by
9 ablation (net surface mass balance equals zero) (Porter 1975, Cogley et al., 2011). ELA can
10 be estimated by fitting a curve to data representing surface mass balance as a function of
11 altitude or a mass balance profile (Cogley et al., 2011). Also it is possible to estimate a
12 climatic ELA as an average of ELA during 30 or more years (Bakke and Nesje, 2011). In
13 this sense the most appropriate definition for a climatic ELA is the steady-state ELA or
14 long term ELA that could be estimated by modelling (Cogley et al., 2011). Fluctuations of
15 ELA have been extensively used in paleoclimatic reconstructions because the ELA is
16 primarily controlled by temperature and precipitation (Porter, 1975, Sagredo et al., 2014).

17 In this paper, we explore the differences in the climatic ELA between the MH and the pre-
18 industrial (PI, hereafter) conditions, using a degree day model with data based on
19 Paleoclimate Modelling Intercomparison Project 2 (PMIP2) climate models output in the
20 Southern Alps in New Zealand and Patagonian Andes in South America (Fig. 1). Therefore
21 this study goes a further step towards linking PMIP2 model simulations, and hence orbital
22 forcing, with the MH glacial record, by explicitly calculating the regional ELAs in
23 Patagonia and New Zealand at 6000 yr B.P. The ELA difference between the PI and MH
24 provides information on the scale of glacier change at this key time.

25

26 **2 Data and methods**

27 **2.1 Experimental setup**

28 With the aim of obtaining comparable results we use a glacier mass balance model forced
29 with Paleoclimate Modelling Intercomparison Project 2 (PMIP2) models for both periods,

1 MH and PI. In the next sections we explain both, the model and the data. General approach
2 consists in resize all PMIP2 models output to a resolution of 0.5° using linear interpolation.
3 Due to the coarse resolution of the PMIP2 models, and the regional nature of this study, we
4 used the ELA as a general indicator of glacier behavior as we are not considering individual
5 glaciers and their specific responses to climatic variations. For each grid point we obtained
6 surface mass balance as a function of altitude. From this mass balance profile we obtained
7 thus a regional ELA.

8 We applied the same procedure for both time slices (mid-Holocene and pre-Industrial) and
9 focus in the difference between the two periods.

10

11 **Glacier Mass Balance Model**

12 We applied a simple glacier mass balance model to explore the regional differences in the
13 ELA between the MH and the PI in the southern mid-latitudes.

14 Degree-day models, as used in this study, have previously been applied for palaeoclimate
15 studies using data from general circulation models (GCM). As examples, Hostetler and
16 Clark (2000) used data from GENESIS (v. 2.01) simulations and inferred ELA positions
17 from mass balance profile curves for the LGM on tropical glaciers. Rupper et al. (2009)
18 also applied this kind of model to the region of Central Asia, using data from re-analysis
19 NCEP-NCAR for the present and data from general circulation models of the phase I of
20 PMIP for the Holocene. The aim was to reconcile Holocene glacier history with climate
21 by quantifying the change in ELA for simulated changes in Holocene climate.

22 Details of the glacier mass balance model, which has been previously applied to Franz
23 Josef glacier, in New Zealand's Southern Alps, can be found in Anderson et al. (2006) and
24 are briefly described here. This model calculates the mass balance gradient for any specific
25 location, based on daily data of temperature and precipitation as a function of elevation.
26 Elevation in the model is defined for each grid point from 0 to 4000 m above sea level (asl)
27 with steps of 20 m. For each elevation, the mass balance is calculated based on:

$$28 \quad \dot{m}(t, z) = \dot{c}(t, z) + \dot{a}(t, z) \quad (1)$$

29 Where \dot{m} is the mass balance rate, \dot{c} the accumulation rate and \dot{a} the ablation rate at time t

1 and elevation z .

2 In glacier mass balance model, accumulation is defined as the portion of the daily
3 precipitation that falls as snow when the daily average temperature is below certain
4 temperature threshold (T_{crit}). Previous studies have considered T_{crit} being in the range of
5 0°C to 2°C (Radic and Hock, 2011). Therefore, water equivalent (w.e.) accumulation is
6 calculated based on the daily information of mean temperature (T_{mean}) and total daily
7 precipitation (p_d), and calculated as:

$$8 \quad c(t, z) = \delta_m p_d \begin{cases} \delta_m = 1, & T_{mean} < T_{crit} \\ \delta_m = 0, & T_{mean} \geq T_{crit} \end{cases} \quad (2)$$

9 In this case, T_{crit} was assumed as 1°C (Anderson et al., 2006).

10 In the middle-latitudes, the ablation process is mainly controlled by melting and runoff
11 (Rupper and Roe 2008). Temperature is a good predictor of melt because incoming
12 longwave radiation and turbulent heat fluxes are important terms in the energy balance that
13 are closely related to air temperature (Ohmura, 2001; Oerlemans, 2001). The other major
14 component of the energy balance, shortwave radiation, is also closely correlated to air
15 temperature.

16 Ablation in the model is proportional to the mean daily temperature, and occurs for values
17 above 0°C (Braithwaite, 1985; Hock, 2005). In this study, we calculated ablation
18 using T_{mean} when this is positive:

$$19 \quad T_d^+(t, z) = \begin{cases} (T_{mean}(t, z) - 0), & T_{mean} > 0^{\circ}\text{C} \\ 0, & T_{mean} \leq 0^{\circ}\text{C} \end{cases} \quad (3)$$

20 Where T_d^+ is a positive daily temperature.

21 Ablation is calculated by multiplying the T_d^+ by a factor that relates temperature and
22 ablation, the degree day factor (DDF). The DDF ($\text{mm w.e. d}^{-1} \text{C}^{-1}$) corresponds to the
23 amount of melting (of ice and snow) per day, which occurs when temperatures are higher
24 than 0°C . This parameter shows great spatial variability and, in general, is higher for ice
25 and lower for snow due to the high albedo of the latter that reduces the absorption of
26 shortwave radiation (Braithwaite, 1995). In this study we use values of 6 and 3 mm w.e. d^{-1}
27 C^{-1} for ice and snow, respectively. These values correspond to the same values used by

1 Woo and Fitzharris (1992) for reconstructing the mass balance for Franz Josef glacier in the
2 Southern Alps. Therefore ablation is estimated by the following relationship:

$$3 \quad a(t, z) = DDF_{ice/snow} * T_d^+(t, z) \quad (4)$$

4 In this study, we use a DDF_{snow} when the snow depth is greater than zero, and DDF_{ice} when
5 the snow depth is equal to zero.

6 Note that, in this study, we assume that temperatures below zero do not contribute to
7 melting (Hock, 2003), and any potential contribution of sublimation to the total ablation is
8 neglected because it is likely small compared to melting.

9 By applying this model at different elevations, we obtain a glacier mass balance curve
10 (specific mass balance with altitude). The ELA occurs where the mass balance equals zero.
11 For the purpose of this study we assumed that some parameters such as temperature and
12 precipitation lapse rates, DDFs and temperature threshold T_{crit} , are constant and equal for
13 both the MH and the PI. Although this might not be strictly correct our focus here is on the
14 relative differences between the two periods rather than absolute values.

15 Given that the model has not previously been used in South America before, a preliminary
16 validation was carried out by comparing model results with existing glacier mass balance
17 data. Unfortunately, very few *in situ* glaciological mass balance measurements exist in
18 southern South America ($> 40^\circ\text{S}$). The most recent published mass balance study in this
19 area was at Mocho glacier, located on the Mocho-Choshuenco volcano ($39^\circ 55' \text{S}$,
20 $72^\circ 02' \text{W}$), which includes the hydrological year 2003/2004 (Rivera et al. 2005).

21 We assessed the performance of the model forced with climatological information coming
22 from a regional climate model at 25-km resolution and forced by the ERA40 reanalyses
23 (PRECIS-ERA40) in Mocho glacier in the Chilean Lake District ($\sim 40^\circ\text{S}$). Because the
24 ERA40 cover the period 1957-2001, we cannot directly compare with the same year
25 analysed in Rivera et al. (year 2005) with the glaciological method (stakes). We therefore
26 run the mass balance model for the closest 10 year period (1980-1989) to the actual
27 observed year, in order to obtain an approximation to the climatological ELA. We use three
28 precipitation lapse rates: 0, 0.00252 and 0.02 mm m^{-1} . This comparison (not shown)
29 showed a reasonable agreement between the observed and modelled ELA, for the low

1 precipitation lapse rates (0 and $0.00252 \text{ mm m}^{-1}$), with a modelled ELA about 100 to 150 m
2 below the observed, which is according to the glacier recession documented for this glacier
3 in the last 30 years (Rivera et al., 2005).

4 5 **2.2 Model inputs: PMIP2**

6 We use daily GCM temperature and precipitation values for computing the degree – day
7 model obtained from simulations carried out under the Paleoclimate Modelling
8 Intercomparison Project 2 (PMIP2), see Braconnot et al. (2007) for model setup and
9 boundary conditions.

10 Although PMIP is currently in its third phase (PMIP3) we used the modelling outputs of
11 PMIP2 given that daily data were not available for the most recent phase when this study
12 began. We analysed 7 models of the PMIP2 initiative (Table 1).

13 We compared the PI outputs with gridded temperature and precipitation data from CRU
14 TS3.10 and CRU TS3.10.01 (Harris et al., 2014) respectively and with weather station
15 observations to assess the climate model results (Supplement Figs. S1 to S4). The glacier
16 mass balance model was driven for 50 years to be able to capture the averaged influence
17 of inter-annual variability, with daily temperature and precipitation data derived from the
18 MH and PI experiments. With the purpose of comparing the ELA between the two
19 periods we calculated the mean mass balance for 50 years. Hence, the ELA calculated for
20 each period corresponds to a long-term or climatic ELA.

21 Temperature data were calculated for different elevations using a standard lapse rate of 6.5
22 $^{\circ}\text{C km}^{-1}$. Due to the scarcity of available precipitation observations at high altitude,
23 especially in Patagonia (Garreaud et al., 2013), precipitation was corrected using a regional
24 mean observed gradient (in mm m^{-1}) in both regions. The observed gradient was obtained
25 using available latitudinal and altitudinal distributions of climate station data in both
26 regions. Fitting the precipitation versus altitude distribution yielded a mean value of
27 $0.00252 \text{ mm m}^{-1}$ in Patagonia and 0.0038 mm m^{-1} in New Zealand. Given that the
28 distribution of precipitation in mountainous regions is difficult to predict even under
29 present-day conditions (Rowan et al., 2014) we use this simple approach to facilitate the

1 process of mass balance modelling. In doing this, we are mindful that we are working at
2 mountain range scale, and that the PMIP2 models do not represent the precipitation
3 gradient very well, especially in the Southern Alps (Supplement Fig. S4). In addition a
4 constant precipitation factor (of 1.55) was also applied to account for the underestimation
5 that low resolution global models have of precipitation at high elevations (e.g. Rojas,
6 2006).

7 The results were averaged over 6 study zones. These zones correspond to: the Chilean Lake
8 District (CLD, approximately between 40°-43° S), Northern Patagonian Icefield (NPI,
9 between 43°-48°S), Southern Patagonian Icefield (SPI, between 48°-53°S) and Cordillera
10 Darwin (CD, between 54°-55°S) in South America, and the northern and southern sector of
11 the South Island of New Zealand (NZN, between 41.5°-43.5°S; and NZS, 43.5°- 46°S,
12 respectively) (Fig. 1). Also we calculated climate differences between MH and PI over
13 these 6 zones using monthly PMIP2 data and tested their significance using a t –test in the
14 case of temperature, and a non-parametric Wilcoxon-Mann-Whitney test in the case of
15 precipitation with a significance level of 95 %.

16

17 **3 Results**

18 **3.1 Climate differences between the mid-Holocene and the pre-industrial**

19 Seasonal temperature differences between the MH and the PI (Fig. 2) are consistent
20 between most models, with temperature anomalies of the same sign and small inter-model
21 spread. Overall, in Patagonia, the models simulate colder conditions during the MH in the
22 austral summer (DJF), autumn (MAM) and winter (JJA), with average temperature
23 anomalies of about -0.2°C, about -0.5°C and about -0.4°C, respectively. During spring
24 (SON) the PMIP2 models shows temperatures 0.2°C warmer.

25 In New Zealand (Fig. 2) the models show colder MH condition in austral autumn (about -
26 0.7°C) and winter (about -0.4°C), and warmer conditions in spring (about 0.3°C). In
27 summer the intermodel spread is larger, so that on average, the temperature anomalies are
28 not significant. In the annual mean, the temperature anomalies for South America and New
29 Zealand are identical (about -0.2°C). These temperature differences reflect the seasonal
30 insolation difference between the two periods. Estimates of precipitation change show less

1 consistency than for temperature (Fig. 3), and in several cases the models show
2 precipitation anomalies of different sign within regions. Nevertheless, there are some
3 regions and seasons for which the models show consistent precipitation changes. For
4 example, during austral summer and autumn the models suggest that the climate was wetter
5 during the MH compared to PI, in the CLD and the Patagonian Icefields. In general all
6 zones exhibit drier winters than the PI; spring was drier in the CLD and NPI, somewhat
7 wetter in the SPI and CD and marginally drier in the New Zealand zones. We find that the
8 CLD was wetter in summer and autumn, no change in winter and dryer in spring. Note that
9 none of the precipitation changes are statistically significant ($p < 0.05$, at 95% confidence
10 interval).

11

12 **3.2 ELA calculations and differences**

13 For ELA calculations, we excluded the FOAM model due to its unsatisfactory simulation
14 of the PI climate results (Supplement Figs. S1 to S4). The spatial distribution of the PI
15 mean ELA based on six PMIP2 models in Patagonia (Fig. 4), shows that the ELA values
16 are higher in the northern section of the study area, with maximum values above 2000 m asl
17 (mean value of 1800 m asl) in the CLD. To the south, the ELA decreases gradually,
18 reaching altitudes below 1000 m asl in SPI (mean value of 960 m asl) and CD (mean value
19 of 840 m asl, see Table 2). Our results also show that, in general, the inter-model variability
20 (one standard deviation) of the ELA estimation is small. One exception is the inter-model
21 variability observed in the SPI, where the maximum standard deviation is 250 m (mean
22 value of 140 m), in a region with mean ELA of about 950 m asl.

23 PI ELA estimates in New Zealand (Fig. 5) are higher in the northern part of South Island
24 (maximum values around 1800 m asl), and slowly decrease to values of 1400 m asl at the
25 southern tip of South Island (Table 2). These modelled values fall within the range of PI
26 ELAs reconstructed from moraine evidence in the South Island (Lorrey et al. 2013). The
27 intermodel spread evaluated with the standard deviation is small in the northern part (148
28 m). South of 43°S, the intermodel spread becomes larger, with values between 150-180 m
29 on the western flank and up to 200 m on the eastern flank of the Southern Alps. The mean
30 value in this zone is 1530 m asl (Table 2).

1 As for the multi model mean ELA differences, in Patagonia (Fig. 6a) and in the Southern
2 Alps (Fig. 6) the ELA was lower during the MH compared to PI, however the magnitude of
3 change is relatively small: in Patagonia the mean difference is ~20 m in all zones, in the
4 Southern Alps is ~30 m in both zones. Besides the small estimated ELA variations, it is
5 important to highlight the consistency between ELA differences calculated by the PMIP2
6 models. In the Southern Alps, all of the six models indicate a negative sign in the ELA
7 differences between the MH and the PI (Fig. 6). In Patagonia at least four models show
8 negative differences between MH and the PI in almost the entire domain, with five models
9 showing a lower ELA during the MH in some parts of the CLD and SPI zones and six
10 models showing the same result in the west coast of the SPI zone (Fig. 6).

11

12 **4 Discussion**

13 **4.1 Difference between mid-Holocene and pre-industrial climates**

14 Rojas and Moreno (2011) evaluated the full PMIP2 MH simulations for the climatic
15 conditions in Patagonia and New Zealand. They found that both regions received less
16 precipitation during a colder accumulation season, and more precipitation during a warmer
17 ablation season. Therefore they suggested, on a qualitative basis, that the temperature and
18 precipitation anomalies could effectively lead to larger glacier during the MH and hence
19 explain Neoglaciation in both regions.

20 This paper goes a step further towards understanding the effects of climatic conditions on
21 glaciers and neoglaciations, and used those conditions to drive a glacier mass balance
22 model.

23 The differences in temperatures between the MH and the PI found in this study are similar
24 to those determined by Ackerley and Renwick (2010) for New Zealand, as well as Rojas
25 and Moreno (2011) for South America and New Zealand. Both studies analyzed data from
26 PMIP2 models, but used a different subset of models. Ackerley et al. (2013) use a regional
27 simulation of higher spatial resolution to simulate the MH climate, and also find a similar
28 temperature pattern found in this study. Given that all these studies indicate that the MH
29 was cooler than the PI in the autumn months and a warming in the spring months, we

1 conclude that the temperature signals are robust across different subset of PMIP2
2 simulations for the MH.

3 Our results indicate mostly wetter conditions during summer (DJF) and drier condition in
4 winter (JJA), in accordance with Rojas and Moreno (2011). For the autumn (MAM) and
5 spring (SON) seasons there is dipole-like signal, with positive precipitation anomalies in
6 the northern regions and drier conditions in the southern regions in MAM and the opposite
7 for SON. These results are also in fair accordance with Rojas and Moreno (2011). In the
8 New Zealand case, we find large inter-model spread between seasons, except during JJA
9 where we find a clear drier condition. Precipitation changes are slightly different than those
10 shown in Ackerly and Renwick (2010), which in turn do not agree with Rojas and Moreno
11 (2011) results. In summary, we found small changes in precipitation and large inter-modal
12 spread, so that existing studies discussed here give slightly different results.

13 **4.2 Differences between mid-Holocene and pre-industrial ELAs**

14 We observe that the mass balance model applied to Patagonia and New Zealand is able to
15 capture the expected differences in the climatological ELA associated with the climate
16 conditions estimated for the MH and the PI. Our results show that during the MH the ELA
17 could have been between 20-30 m lower than during the PI in Patagonia and New Zealand.

18 We propose that the results of the modelled ELA differences can be explained mainly by
19 the significant and consistent differences in modelled temperatures observed. The impact of
20 the precipitation anomalies are more difficult to assess, given that the climate data is
21 heterogeneous. This suggestion is consistent with the idea that glaciers from mid-latitudes
22 are more sensitive to changes in temperature than to changes in precipitation (Anderson and
23 Mackintosh, 2006). Moreover, we suggest that the observed differences in climatological
24 ELA are mainly driven by changes in the annual temperature cycle in these temperate
25 regions. In Patagonia, ablation dominantly occurs between September and March (spring
26 and summer months); whereas accumulation occurs from April to August (autumn and
27 winter months) (Rodbell et al., 2009). In New Zealand most of the ablation occurs between
28 November and April (summer and parts of spring and autumn), whereas accumulation
29 occurs from May to October (winter and parts of autumn and spring). However both
30 regions experience significant interannual variations, where accumulation or ablation

1 sometimes persists for longer period.

2 In Patagonia and New Zealand the lower summer temperatures observed during the MH
3 imply less energy input and hence lower amounts of ablation. Although the opposite
4 happens in spring, where the higher temperatures of the MH indicate greater ablation, we
5 suggest that this change was not sufficient to balance the impact of the lower summer
6 temperature on the mass balance. In addition, the lower temperatures observed during
7 autumn and winter would increase the percentage of precipitation falling as snow rather
8 than rain during the MH, as hypothetically suggested by Sagredo and Lowell (2012) and
9 Rodbell et al. (2009). This is particularly critical in the Southern Alps, where a significant
10 portion of the modern precipitation falls roughly at the elevation of the ELA. A temperature
11 drop in this area would result in an increment in snow precipitation (Rother and
12 Shulmeister, 2006). This can be particularly important in autumn and spring, when
13 temperatures in the vicinity of the ELA are typically -1 to 2 °C. Additionally precipitation
14 during winter is higher during the MH in almost all the PMIP2 models in all zones (Fig. 3),
15 this also contributes to accumulation and therefore a lower ELA in the MH with respect to
16 PI.

17 **4.3 ELA sensitivity to model parameters**

18 We performed sensitivity runs to increase the robustness of the modelling results in the
19 Patagonian and Southern Alps sectors. This motivated by the small differences in modelled
20 ELAs and the lack of constraints on important parameters owing to the scarcity of
21 measurements, especially in Patagonia. We investigated the sensitivity of ELA to the
22 precipitation lapse rate and the Degree Day Factor (DDF) of snow and ice.

23 We assessed precipitation lapse-rate values of 0, 0.001 and 0.02 mm m⁻¹ considering the
24 observed precipitation gradient in Patagonia and the Southern Alps of New Zealand
25 (0.00252 and 0.0038 mm m⁻¹ respectively). The sensitivity in the ELA difference to the
26 precipitation lapse rate has a maximum of 15 m in the northern part of Southern Island
27 (Fig.7) (glaciers do not exist in this zone). At the latitude of the northern glaciers of the
28 Southern Alps (approximately 43°S) the sensitivity is close to 10 m. Sensitivity declines
29 southward (see Fig. 7). In Patagonia (Fig. 8), the Chilean Lake District has a maximum
30 sensitivity of 6 m. This value is lower in the Northern Patagonia Icefield zone (2 to 3 m)

1 and close to 5 m in the Southern Patagonia Icefield. From both Figures it is clearer that in
2 almost all the study zone, for higher precipitation lapse rates values, the ELA differences
3 between the two periods become larger. We therefore conclude that the small ELA
4 differences in Patagonia and Southern Alps are significant and robust to this parameter and
5 therefore the results presented are the most conservative modelled ELA differences.

6 We assessed DDF values of 4, 8 and 10 mm d⁻¹ °C⁻¹ for ice and 2 and 4 mm d⁻¹ °C⁻¹ for
7 snow, within range of theoretical values used in the glacier modelling (3 mm d⁻¹ °C⁻¹ for
8 snow and 6 mm d⁻¹ °C⁻¹ for ice). DDF sensitivity is even lower in Southern Alps with a
9 maximum of 3 m in the northern part and also a reduction in the sensitivity to the south
10 (Fig. 7). In Patagonia sensitivity is 3 to 4 m along the Andes (Fig. 8).

11 **4.4 Comparison of geomorphically-reconstructed ELA and model results**

12 In the following paragraphs we assess our estimates of ELA change against some records of
13 neoglacial activity in both study areas

14 In Lago General Carrera (named Lago Buenos Aires in the Argentinean side, 46° 30' S),
15 central Patagonia, it has been shown that glaciers advanced around 6200 yr B.P. (Douglass
16 et al., 2005). Geomorphic evidence at this site suggests that during this glacial advance the
17 ELA dropped to 1100 m asl, a 300 m difference with respect to the present position
18 estimate for small isolated cirque glaciers. Further evidence of glacier activity is found by
19 Harrison et al. (2012) who determined ages of 5700 yr B.P. for a moraine located to the
20 west of the North Patagonian Icefield (46 ° 36 ' S / 73 ° 57 ' W) associated with San Rafael
21 glacier. Recently Strelin et al. (2014) found evidence for glacier advance between 6000 –
22 5000 yr B.P. based in moraine dating in the east side of Southern Patagonia Icefield (Lago
23 Argentino), specifically associated with the Upsala, Agassiz and Frías glaciers. However, in
24 the latter two studies, ELA differences were not calculated.

25 In the Southern Alps, geomorphic and geochronological evidence suggest that Tasman and
26 Mueller glaciers (43°50' S/170°E) advanced around 6740 ±160 yr B.P. (Schaefer et al.,
27 2009, age updated in Putnam et al., 2012). Putnam et al. (2012) demonstrated that a MH
28 glacial advance also occurred at Cameron glacier (~43°20'S/171°E) at 6890 ± 190 yr B.P.,
29 suggesting a regional event. In Putnam et al. (2012), ELA estimated for MH was ~140 m
30 lower than present, and 110 m lower than present 180±48 years ago. This suggests a fairly

1 modest change (~30 m) between the MH and PI, consistent with the results of the ELA
2 modelling in this work. While there is a systematic difference between the PI ELA
3 calculated by the model and modern observations, it is clear that relative changes in ELA
4 are very similar between our work and the estimates by Putnam et al. (2012).

5 The qualitative agreement in the direction of change between our modelling results and
6 geomorphic studies in these regions, despite absolute differences that are significantly
7 smaller (in the order of the tens of meters), lead us to conclude that the mass balance
8 modelling accounts for some but not all of the climatic differences between this two
9 periods.

10 Several caveats in our study account for more quantitative agreement in the absolute value
11 of the ELA. 1) We compare the MH simulations with PI conditions, which are different
12 from late 20th century climate. Reconstructions based on geologic evidence, on the other
13 hand, are compared against late 20th century conditions. 2) Glacier advances during the
14 mid-Holocene did not necessarily coincide with a precise time-slice, namely 6000 yr B.P.
15 3) The spatial scale of individual glaciers and the coarse resolution of climate models
16 hinder a direct comparison. 4) Important uncertainties are present in model parameters,
17 especially those related with the spatial distribution of precipitation and degree day factors.
18 5) The magnitude of the glacier expansion and mass balance from a given ELA change
19 depends on local conditions and characteristics of the glaciers, for example, glacier bed
20 slope and hypsometry (Oerlemans, 2012; De Angelis, 2014). Glacier bed slope is a primary
21 control on length sensitivity (Oerlemans, 2012) where a glacier with a gentle bed slope,
22 such as Upsala glacier in South Patagonia Icefield, shows a high length sensitivity to ELA
23 changes, estimated at ~-50 metres of glacier length per metre of ELA increase (Oerlemans,
24 2012). With this in mind we expected large change of the accumulation and ablation areas
25 even if the ELA oscillation is small (Mercer, 1965, Furbish and Andrews, 1984). In
26 contrast, the steep Franz Josef Glacier shows a much smaller length sensitivity of ~-10
27 metres of glacier length per metre of ELA increase. Glacier hypsometry is also an
28 important control on the sensitivity of mass balance to change in ELA, according to De
29 Angelis (2014) glaciers where the bulk of the area is located below the ELA are subject to
30 the largest changes of mass balance for any given changes in ELA. Considering all these
31 aspects and limitations of the glacier mass balance model, we highlight agreement among

1 both, the sign of change and regional homogeneity within and between both study regions.
2 This in-phase ELA response in Patagonia and New Zealand's South Island, is also in
3 agreement with glacier fluctuations observed during the 20th century where glaciers seem
4 to be in phase to similar climate forcing (Fitzharris et al., 2007).

5 6 **5 Conclusions**

7 A glacier mass balance model forced with PMIP2 simulations showed that southern mid-
8 latitude glacier ELAs during the mid-Holocene (MH) were lower compared to pre-
9 industrial (PI) conditions. The robustness of these results are evaluated by using six
10 different climate model data to run the mass balance model, as well as additional
11 simulations varying a number of not well constrained parameters of the model such as the
12 precipitation lapse-rate and the snow and ice degree day factors. The results of those
13 sensitivity simulations showed that the ELA differences, although small, had always the
14 same sign in New Zealand i.e., lower ELAs during the MH compared to PI and in most of
15 the models in Patagonia. We have therefore confidence that climatic conditions, as
16 simulated by six PIMIP2 models for MH conditions could lead to larger glaciers extents
17 during this period. The main forcing of the modelled ELA differences are temperature
18 differences. Significantly colder conditions during the summer, autumn and winter months
19 prevailed during the MH compared to the PI. In contrast, modelled precipitation changes
20 were small and with disagreement between models for the sign of change. Given that ELAs
21 for the MH were consistently lower despite the range of precipitation data they were forced,
22 our ELA results underline the evidence that temperate glaciers show a greater sensitivity to
23 temperature changes (Anderson and Mackintosh, 2006).

24 Cooler temperatures during the MH would have affected glacier mass balance during both
25 summer and winter. In summer and early autumn in the MH, less energy would be
26 available for ablation, whereas from autumn to late winter, lower temperatures would cause
27 a larger portion of precipitation to fall as snow, resulting in higher accumulation in the MH
28 with respect to the PI, as well as a higher surface albedo which reduces the amount of short-
29 wave radiation available for melt.

30 This study provides new insights towards understanding southern hemisphere mid-

1 Holocene glacier conditions, demonstrating that orbital forcing inducing relatively coherent
2 temperature changes are consistent with a hemispheric pattern of larger glacier extent at
3 MH compared to the PI period

4

5 **Acknowledgments**

6 We acknowledge the international modelling groups for providing their data for analysis,
7 the Laboratoire des Sciences du Climat et de l'Environnement (LSCE) for collecting and
8 archiving the model data. The PMIP2/MOTIF Data Archive is supported by CEA, CNRS,
9 the EU project MOTIF (EVK2-CT-2002- 00153) and the Programme National d'Etude de
10 la Dynamique du Climat (PNEDC). C. Bravo acknowledges the support of CONICYT
11 magister scholarship. The Millennium Nucleus NC120066 and CR2 N15110009 supported
12 this investigation. M. Rojas and P.I. Moreno received support by FONDECYT grant #
13 1131055. E. Sagredo acknowledges support by FONDECYT Iniciación Grant # 11121280
14 and CONICYT Grant USA-2013-0035. A.N. Mackintosh and B.M. Anderson acknowledge
15 financial support from Victoria University Foundation Grant, "Antarctic Research Centre
16 Climate and Ice-Sheet Modelling". We would like to thank to A.V. Rowan, one anonymous
17 referee and J. Ubeda for their constructive and useful comments. This work is a
18 contribution towards the SHAPE (Southern Hemisphere Assessment of
19 PalaeoEnvironments) project, which is supported by the International Union for Quaternary
20 Research.

21

22 **References**

23 Ackerley, D. and Renwick, A.: The Southern Hemisphere semiannual oscillation and
24 circulation variability during the Mid-Holocene, *Clim. Past*, 6, 415-430, 2010.

25 Ackerley, D., Lorrey, A., Renwick, J., Phipps, S., Wagner, S., and Fowler, A.: High
26 resolution modelling of mid-Holocene New Zealand climate at 6000 yr B.P., *Holocene*, 23,
27 1272-1285, 2013.

28 Anderson, B. and Mackintosh, A.: Temperature change is the major driver of late-glacial
29 and Holocene glacier fluctuations in New Zealand, *Geology*, 34, 121-124, 2006.

1 Anderson, B., Lawson, W., Owen, I., and Goodsell, B.: Past and future mass balance of
2 ‘KaRoimata o Hine Hukatere’ Franz Josef Glacier, New Zealand, *J. Glaciol*, 52, 597-607,
3 2006.

4 Aniya, M.: Holocene glacial chronology in Patagonia: Tyndall and Upsala glaciers, *Arctic*
5 *Alpine Res.*, 27, 311-322, 1995.

6 Aniya, M.: Holocene glaciations of Hielo Patagónico (Patagonia Icefield), South America:
7 A brief review, *Geochemical Review*, 47, 97-105, 2013.

8 Bakke, J. and Nesje, A.: Equilibrium-Line Altitude (ELA), in: *Encyclopedia of Snow, Ice*
9 *and Glaciers*, edited by: Singh, V., Singh, P., and Haritashya, U., Springer, the Netherlands,
10 268– 277, 2011.

11 Braconnot, P., Otto-Bliesner, B., Harrison, S., Joussaume, S., Peterchmitt, J.-Y., Abe-
12 Ouchi, A., Crucifix, M., Driesschaert, E., Fichefet, Th., Hewitt, C. D., Kageyama, M.,
13 Kitoh, A., Lâiné, A., Loutre, M.-F., Marti, O., Merkel, U., Ramstein, G., Valdes, P., Weber,
14 S. L., Yu, Y., and Zhao, Y.: Results of PMIP2 coupled simulations of the Mid-Holocene
15 and Last Glacial Maximum - Part 1: experiments and large-scale features, *Clim. Past*, 3,
16 261-277, doi:10.5194/cp-3-261-2007, 2007.

17 Braithwaite, R.: Calculation of degree-days for glacier–climate research, *Zeitschrift für*
18 *Gletscherkunde und Glazialgeologie* 20, 1-8, 1985.

19 Braithwaite, R.: Positive degree-day factors for ablation on the Greenland ice sheet studied
20 by energy-balance modelling, *J. Glaciol* 41, 153-160, 1995.

21 Clapperton, C. and Sugden, D.: Holocene glacier fluctuations in South America and
22 Antarctica, *Quaternary Sci. Rev.*, 7, 185-198, 1988.

23 Cogley, J. G., Hock, R., Rasmussen, L. A., Arendt, A. A., Bauder, A., Braithwaite, R. J.,
24 Jansson, P., Kaser, G., Moller, M., Nicholson, L., and Zemp, M.: Glossary of Glacier Mass
25 Balance and Related Terms, IHP-VII Technical Documents in Hydrology No. 86, IACS
26 Contribution No. 2, UNESCO-IHP, Paris, 2011.

27 De Angelis, H.: Hypsometry and sensitivity of the mass balance to changes in equilibrium-
28 line altitude: the case of the Southern Patagonia Icefield, *Ann Glaciol*, 60, 14-28, 2014.

1 Douglass, D., Singer, B., Kaplan, M., Ackert, R., Mickelson, D., and Caffee, M.: Evidence
2 of early Holocene glacial advances in southern South America from cosmogenic surface-
3 exposure dating, *Geology* 33, 237-240, 2005.

4 Doughty, A., Scafefer, J., Putnam, A., Denton, G., Kaplan, M., Barrell, D., Andersen, B.,
5 Kelley, S., Finkel, R., and Schwartz, R.: Mismatch of glacier extent and summer insolation
6 in Southern Hemisphere mid-latitudes, *Geology*, 43, 407- 410, 2015.

7 Fitzharris, B., Clare, G., and Renwick, J.: Teleconnections between Andean and New
8 Zealand glaciers, *Global Planet. Change*, 59, 159-174, 2007.

9 Fletcher, M. and Moreno, P.: Have the Southern Weterlies changes in a zonally symmetric
10 manner over the last 14000 years? A hemisphere-wide take on a controversial problem,
11 *Quatern. Int.*, 254, 32-46, 2012.

12 Furbish, D. and Andrews, J.: The use of hypsometry to indicate long-term stability and
13 response of valley glaciers to changes in mass transfer, *J. Glaciol*, 30, 192-211, 1984.

14 Garreaud, R., Lopez, P., Minvielle, M., and Rojas, M.: Large Scale Control on the
15 Patagonia Climate, *J. Climate*, 26, 215-230, 2013.

16 Gellatly, A., Chinn, T. and Röthlisberger, F.: Holocene glacier variation in New Zealand: a
17 review, *Quaternary Sci. Rev.*, 7, 227-242, 1988.

18 Harris, I., Jones, P., Osborn, T., and Lister, D.: Updated high-resolution grids of monthly
19 climatic observations – the CRU TS3.10 Dataset, *Int. J. Climatol.*, 34, 623- 642, 2014.

20 Harrison, S., Glasser, N., Duller, G., and Jansson, K.: Early and mid-Holocene age for the
21 Tempanos moraine, Laguna San Rafael, Patagonian Chile, *Quaternary Sci. Rev.*, 31, 82-
22 92, 2012.

23 Hock, R.: Temperature index melt modelling in mountains areas, *J. Hydrol.*, 282, 104-115,
24 2003.

25 Hock, R.: Glacier melt: a review of processes and their modelling, *Prog. Phys. Geog.*, 29,
26 362-391, 2005.

27 Hostetler, S., and Clark, P.: Tropical climate at the Last Glacial Maximum inferred from
28 glacier mass-balance modelling, *Science*, 290, 1747-1750, 2000.

1 Kaplan, M., Schaefer, J., Denton, G., Doughty, A., Barrel, D., Chinn, T., Putnam, A.,
2 Andersen, B., Mackintosh, A., Finkel, R., Schwartz, R., and Anderson, B.: The anatomy of
3 long-term warming since 15 ka in New Zealand based on net glacier snowline rise,
4 *Geology*, 41, 887-890, doi:10.1130/g34288.1, 2013.

5 Lorrey, A., Fauchereau, N., Stanton, C., Chappell, P., Phipps, S., Mackintosh, A., Renwick,
6 J., Goodwin, I., Fowler, A. (2013). The Little Ice Age climate of New Zealand
7 reconstructed from Southern Alps cirque glaciers: A synoptic type approach. *Climate*
8 *Dynamics*, 42(11-12): 3039 - 3060. doi:10.1007/s00382-013-1876-8.

9 Mayewski, P., Rohling, E., Stager, J., Karlén, W., Maasch, K., Meeker, L., Meyerson, E.,
10 Gasse, F., Van Kreveld, S., Holmgren, K., Lee-Thorp, J., Rosqvist, G., Rack, F.,
11 Staubwasser, M., Schneider, R., and Steig, E.: Holocene climate variability, *Quaternary*
12 *Res.*, 62, 243 -255, 2004.

13 Mercer, J.: Glacier variations in southern Patagonia, *Geogr. Rev.*, 55, 390- 413, 1965.

14 Mercer, J.: Holocene glacier variation in southern South America, *Striae*, 18, 35-40, 1982.

15 Moreno P., Francois, J.P., Villa-Martinez, R., and Moy, C.: Covariability of the Southern
16 Westerlies and atmospheric CO₂ during the Holocene, *Geology*, 38, 727-730, 2010.

17 Oerlemans, J.: *Glaciers and climate change*. A.A. Balkema Publisher, Lisse, 2001.

18 Oerlemans, J.: Linear modelling of glacier length fluctuations, *Geogr. Ann. A.*, 94, 183-
19 194. doi: 10.1111/j.1468-0459.2012.00469.x, 2012.

20 Ohmura, A.: Physical basis for the Temperature-Based Melt-Index Method, *J. Appl.*
21 *Meteorol.*, 40, 753-761, 2001.

22 Porter, S.: Onset of Neoglaciation in Southern Hemisphere, *J. Quaternary Sci.*, 15, 395-
23 408, 2000.

24 Porter, S. and Denton, G.: Chronology of Neoglaciation in the North American Cordillera,
25 *Am. J. Sci.*, 265, 177- 210, 1967.

26 Porter, S.: Equilibrium line altitudes of late Quaternary glaciers in the Southern Alps, New
27 Zealand, *Quaternary Res.*, 5, 27-47, 1975.

28 Putnam, A., Schaefer, J., Denton, G., Barrel, D., Finkel, R., Anderson, B., Schwartz, R.,

1 Chinn, T., and Doughty, A.: Regional climate control of glaciers in New Zealand and
2 Europe during the pre-industrial Holocene, *Nat. Geosci.* 5, 627-630,
3 Doi:10.1038/ngeo1548, 2012.

4 Radic, V. and Hock, R.: Regionally differentiated contribution of mountain glaciers and ice
5 caps to future sea level rise, *Nat. Geosci.*s, 4, 91- 94, 2011.

6 Rivera, A., Bown, F., Casassa, G., Acuña, C., and Clavero, J.: Glacier shrinkage and
7 negative mass balance in the Chilean Lake District (40°S). *Hydrolog Sci J* 50, 963- 974,
8 2005.

9 Rodbell, D., Smith, J., and Mark. B.: Glaciation in the Andes during Lateglacial and
10 Holocene, *Quaternary Sci. Rev.*, 28, 2165-2212, 2009.

11 Rojas, M.: Multiple Nested Regional Climate Simulations for Southern South America:
12 Sensitivity to Model Resolution. *Mon. Weather Rev.*, 134, 2208-2223, 2006.

13 Rojas, M., Moreno, P., Kageyama, M., Crucifix, M., Hewitt, C., Abe, A., Ohgaito, R.,
14 Brady, E., and Hope, P.: The Last Glacial Maximum in the Southern Hemisphere in PMIP2
15 simulations. *Clim. Dynam.*, 32, 525-548, 2009.

16 Rojas, M. and Moreno, P.: Atmospheric circulation changes and neoglacial conditions in
17 the Southern Hemisphere mid-latitudes: insights from PMIP2 simulation at 6 kyr, *Clim.*
18 *Dynam.*, 37, 357- 375, 2011.

19 Rother, H. and Shulmeister, J.: Synoptic climate change as a driver of late Quaternary
20 glaciations in the mid-latitudes of the Southern Hemisphere. *Clim. Past*, 2, 11-19, 2006.

21 Rowan, A., Brocklehurst, S., Schultz, D., Plummer, M., Anderson, L. And Glasser, N.: Late
22 Quaternary glacier sensitivity to temperature and precipitation distribution in the Southern
23 Alps of New Zealand, *J Geophys Res Earth Surf*, 119, 1064-1081, 2014.

24 Rupper, S. and Roe, G.: Glacier change and regional climate: A mass and energy balance
25 approach, *J. Climate*, 21, 5384-5401, 2008

26 Rupper, S., Roe, G., and Gillespie, A.: Spatial patterns of Holocene glacier advance and
27 retreat in Central Asia, *Quaternary Res.*, 72, 337- 346, 2009.

28 Sagredo, E. and Lowell, T.: Climatology of Andean glaciers: A framework to understand

1 glacier response to climate change, *Global Planet. Change*, 86-87, 101-109, 2012.

2 Sagredo, E., Rupper, S., and T. Lowell, T.: Sensitivities of the equilibrium line altitude to
3 temperature and precipitation changes along the Andes, *Quaternary Res.*, 81, 355-366,
4 2014.

5 Schaefer, J., Denton, G., Kaplan, M., Putman, A., Finkel, R., Barrel, D., Anderson, B.,
6 Schwartz, R., Mackintosh, A., Chinn, T., and Schluchter, C.: High-frequency Holocene
7 glacier fluctuation in New Zealand differs from the Northern signature, *Science*, 324, 622-
8 625, 2009.

9 Solomina, O., Bradley, R., Hodgson, D.A., Ivy-Ochs, S., Jomelli, V., Mackintosh, A.,
10 Nesje, A., Owen, L., Wanner, H., Wiles, G.C., and Young, N.E.: Holocene glacier
11 fluctuations. *Quaternary Sci. Rev.*, 111,9-34, 2015.

12 Strelin, J., Kaplan, M., Vandergoes, M., and Denton, G.: Holocene glacier history of the
13 Lago Argentino basin, Southern Patagonian Icefield, *Quaternary Sci. Rev.*, 101, 124-145,
14 2014.

15 Woo, M and B. Fitzharris, B.: Reconstruction of mass balance variations for Franz Josef
16 Glacier, New Zealand, 1913-1989, *Arctic Alpine Res.*, 24 (4), 281-290, 1992.

17 Table 1. PMIP2 models used in this study.

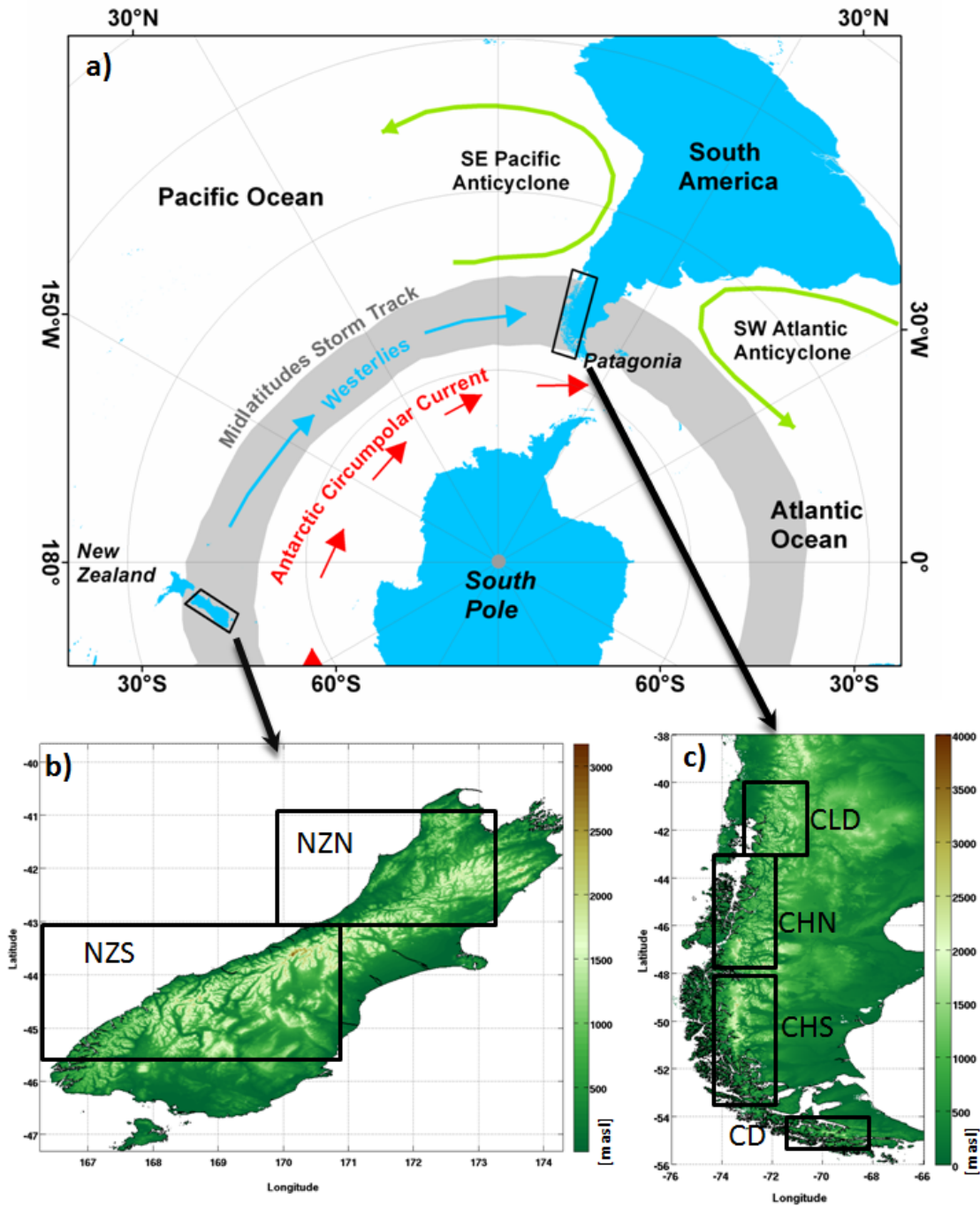
Models	Atmosphere	Vertical	Years of data
--------	------------	----------	---------------

	lon x lat	levels	used
CSIRO-Mk3L-1.1	5.625 x ~ 3.18	18	50
ECHAM5-MPIOM1	3.75 x 2.5	20	50
FOAM	7.5 x 4.5	18	50
MIROC3.2	2.8 x 2.8	20	50
MRI-CGCM2.3.4fa	2.8 x 2.8	30	50
MRI-CGCM2.3.4nfa	2.8 x 2.8	30	50
UBRIS-HadCM3M2	3.75 x 2.5	19	50

1 Table 2. Mean values of ELA for each zone

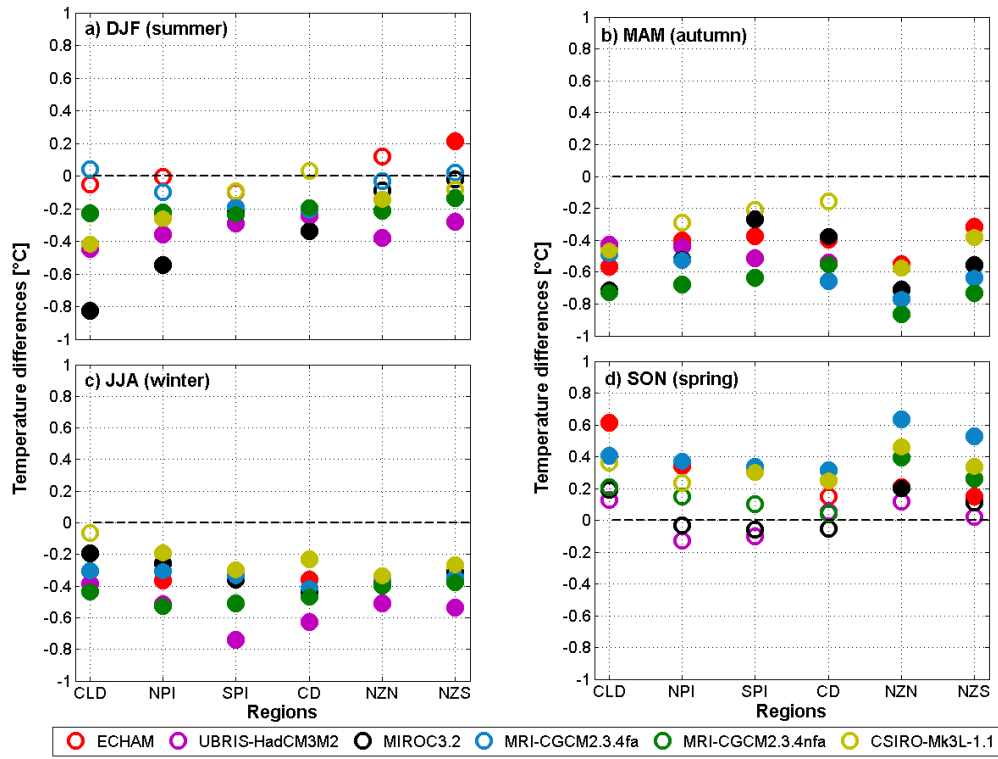
Region	Zones	ELA MH [m asl]	ELA PI [m asl]	Difference [m]
--------	-------	----------------	----------------	----------------

	Chilean Lake District	1776 ± 99	1797 ± 93	-21 ± 6
Patagonia	Northern Patagonia Icefield	1333 ± 125	1354 ± 106	-21 ± 3
	Southern Patagonia Icefield	939 ± 148	956 ± 140	-17 ± 5
	Cordillera Darwin	821 ± 90	839 ± 89	-18 ± 4
	South Island, New Zealand	North	1667 ± 144	1697 ± 148
	South	1501 ± 176	1528 ± 176	-27 ± 6



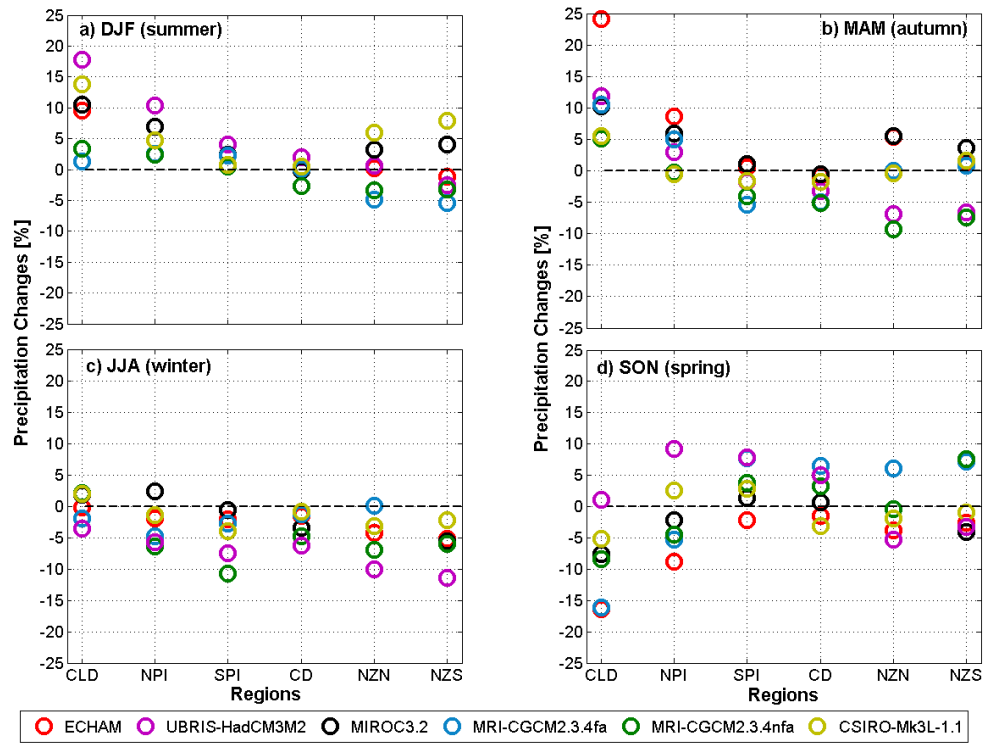
1

2 Figure 1. Study area. (a) Schematic diagram showing some of the main climate
 3 characteristics in the southern mid-latitudes. (b) New Zealand southern island topography
 4 and the two zones of analysis (NZN: New Zealand north, NZS, and New Zealand south).
 5 (c) Patagonia topography and the four zones of analysis (CLD: Chilean Lake District,
 6 CHN: North Patagonian Icefield, CHS: South Patagonian Icefield and CD: Cordillera
 7 Darwin).



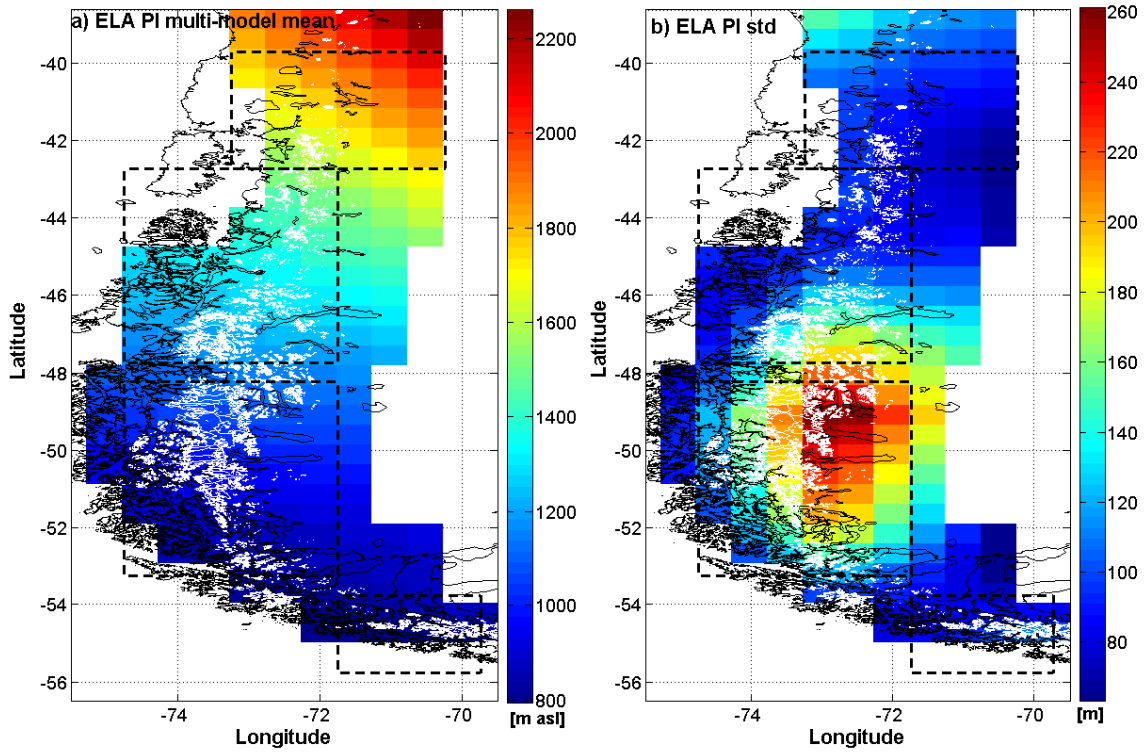
1

2 Figure 2. Temperature differences: Mid-Holocene minus Preindustrial, over the 6 zones of
 3 analysis. (a) DJF, (b) MAM, (c) JJA, (d) SON. Filled circles correspond to statistically
 4 significant differences ($p \leq 0.05$).



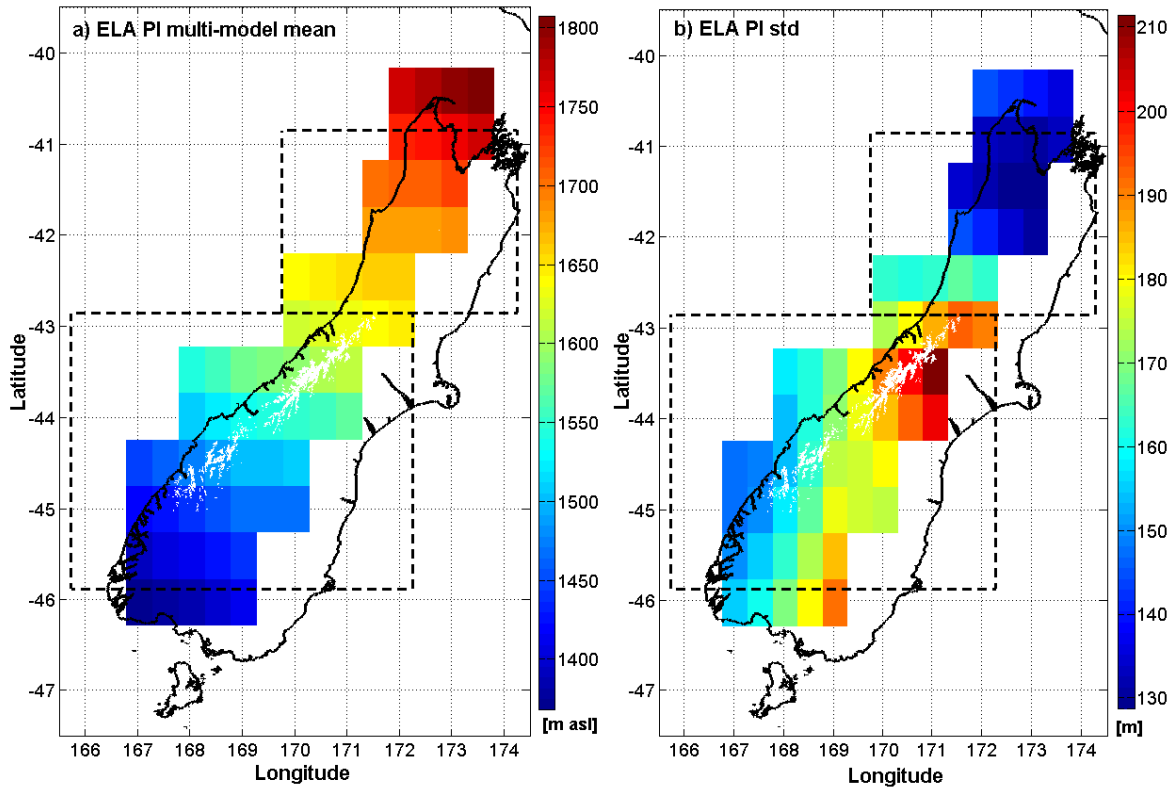
1

2 Figure 3. Precipitation differences: Mid-Holocene minus Preindustrial, over the 6 zones of
 3 analysis. (a) DJF, (b) MAM, (c) JJA, (d) SON. Filled circles correspond to statistically
 4 significant differences ($p \leq 0.05$).



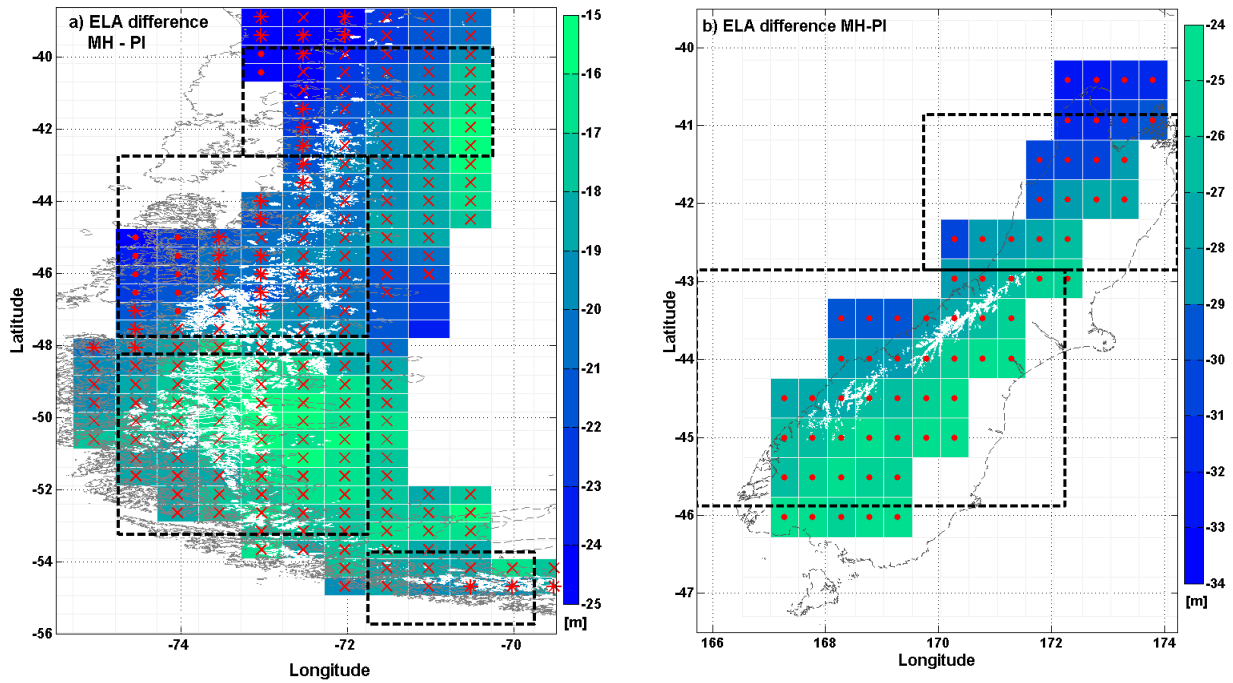
1

2 Figure 4. Spatial distribution of pre-industrial equilibrium line altitude (ELA) in South
 3 America based on six PMIP2 simulations. (a) mean ELA (m asl) and (b) inter-model
 4 variability of the ELA (one standard deviation). White lines correspond to actual glacier
 5 extension according to the Randolph Glacier Inventory (RGI 3.2)



1

2 Figure 5. Spatial distribution of pre-industrial equilibrium line altitude (ELA) in Southern
 3 Island of New Zealand based on six PMIP2 simulations. (a) Mean ELA (m asl) and (b)
 4 inter-model variability of the ELA (one standard deviation). White lines correspond to
 5 actual glacier extension according to the Randolph Glacier Inventory (RGI 3.2)

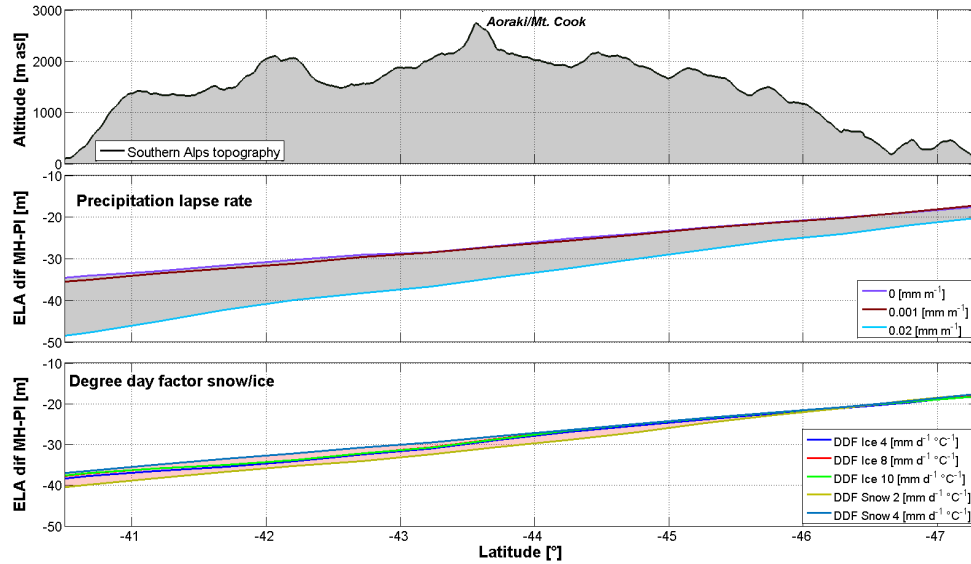


1

2 Figure 6. Mid-Holocene minus pre-industrial equilibrium line altitude differences. Points
 3 indicate that the six models have a negative sign in the differences; asterisks indicate that
 4 five models have a negative sign and crosses indicate that four models have a negative sign.
 5 White lines indicate actual glacier outlines (Randolph Glacier Inventory 3.2). a) Patagonia,
 6 b) New Zealand.

7

8



1

2 Figure 7. Sensitivity of ELA differences in Southern Alps to precipitation lapse rate and
 3 degree day factor of snow and ice. a) Latitudinal topography profile of Patagonia (SRTM 1
 4 km) b) ELA difference sensitivity to precipitation lapse rate and c) ELA difference
 5 sensitivity to degree day factor of snow and ice. Gray and pink areas in b) and c) represent
 6 the range in ELA differences between MH and PI.

7

8

9

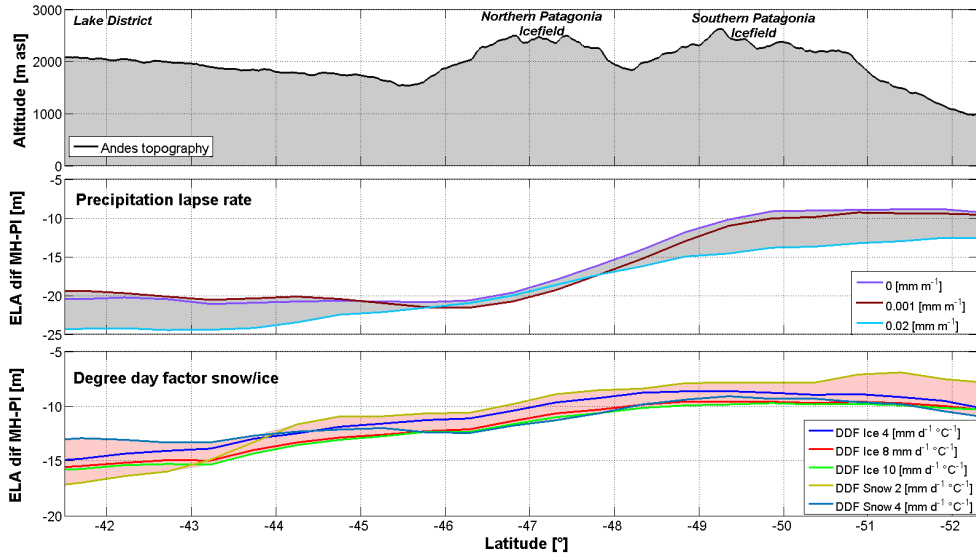
10

11

12

13

14



1

2 Figure 8. Sensitivity of ELA differences in Patagonian Andes to precipitation lapse rate and
 3 degree day factor of snow and ice. a) Latitudinal topography profile of Patagonia (SRTM 1
 4 km) b) ELA differences sensitivity to precipitation lapse rate and c) ELA differences
 5 sensitivity to degree day factor of snow and ice. Gray and pink areas in b) and c) represent
 6 the range in ELA differences between MH and PI.

7

8

9

10